Infrared spectra of carbon nitride films

S.E. Rodil[a],*, A.C. Ferrari[b], J. Robertson[b], S. Muhl[a]

[a]*Instituto de Investigaciones en Materiales, Universidad Nacional Autónoma de México, Apartado Postal 70-360, Coyoacan D.F. 04510, Mexico*
[b]*Engineering Department, Cambridge University, Trumpington Street, Cambridge CB2 1PZ, UK*

Abstract

The assignment of the vibrational modes in amorphous carbon nitride (CN) films is discussed by considering CN films deposited using a variety of methods. The infrared (IR) spectra of CN show three main absorption bands. In hydrogenated CN samples, CH_x and NH_x groups give rise to stretching vibrations at 3000 and 3400 cm^{-1}, respectively. A weaker sharp band is observed approximately 2200 cm^{-1} due to CN–sp^1 bonds. Finally, there is a broad band between 1000 and 2000 cm^{-1}. It is usually stated that the effect of nitrogen into carbon films is to break the symmetry of the sp^2 carbon bonds making the Raman 'G' (graphitic) and 'D' (disorder) modes IR active, so the broad band between 1000 and 2000 cm^{-1} is similar in both IR and Raman spectra. However, it is shown that nitrogen is not necessary to have significant IR activity in the 1000–2000 cm^{-1} region. Also, Raman spectroscopy in carbon is always a resonant process, so that the spectra depend on the excitation energy. Therefore, the similarity of the visible Raman and IR spectra of some CNs is generally a coincidence. We show that the IR broad band in the 1000–2000 cm^{-1} region is an electronic effect and is not due to activation of IR forbidden modes due to symmetry breaking. This explains the IR spectra not only of CN films but also of N-free amorphous carbon films and is related to the presence of the system of delocalized π bonds with increasing conjugation.
© 2002 Elsevier Science B.V. All rights reserved.

Keywords: Infrared spectroscopy; Carbon; Nitrides; Raman scattering; Optical properties; Electron energy loss spectroscopy (EELS)

1. Introduction

The motivation for studying carbon-nitride (CN) compounds has been the search for the super-hard [1] β-C_3N_4, which so far has resulted just a hypothetical phase since no experimental result has demonstrated definitely the existence of such a phase [2–4]. However, amorphous CN compounds are of great importance, both from a scientific and technological point of view. For technology, because many interesting applications are emerging, such as gas sensors [5] or infrared (IR) detectors [6], and scientifically since the interpretation of the experimental results probing the bonding configurations is still under debate.

Carbon and nitrogen are exceptional elements: they are both able to bond in three different hybridisation states. Heteronuclear bonds, in particular, change from the strong C–N and C=N groups, both in chains and heterocyclic rings, to terminating nitrile CN groups [7].

Many studies on CN have been devoted to identify the bonding configurations. One of the most popular techniques is X-ray photoelectron spectroscopy (XPS). However, the interpretation of the results is still controversial [8–10]. Electron energy loss spectroscopy (EELS) has shown that the addition of nitrogen into the carbon network increases the sp^2 fraction, however, only limited work has been devoted to study CN bonding or the N bonding states [11–14]. Another useful technique, although not so easily accessible is X-ray absorption (NEXAFS or XANES). The overall resolution is much better than for EELS, so the fine structure in the π peaks of both the C and N edges can be studied. Recently the correlation between XPS and NEXAFS, has been object of interesting studies [15–18]. In our opinion there is a need for a comparison between a-C:N films and well-known molecules to obtain a greater confidence in the interpretation of the current results. On the other hand, IR and Raman spectroscopy are

*Corresponding author. Tel.: +52-55-56-22-47-34; fax: +52-55-56-16-12-51.
E-mail address: saro36@yahoo.com.mx (S.E. Rodil).

widely available, rapid and non-destructive probes that have been extensively used in the literature. An early interpretation of the main features in the IR spectra was given by Kaufman et al. [19]. Many subsequent papers have used this idea to explain their results, without the necessary critical analysis of their original proposal. The aim of this paper is to propose an alternative and consistent model able to explain the origin of the IR intensity in a-C:N. This contrasts with the ideas of Ref. [19], which were recently challenged by us and other authors [20–23].

We will show how all the measured IR spectra of any a-C:N films can be classified in only 4 different groups. We produced samples for each one of the groups. These samples have been fully characterized in terms of their IR and resonant Raman spectra.

2. Experimental

Hydrogenated and hydrogen free samples were produced using different deposition methods. If no N is introduced, two of the deposition techniques we used, normally produce highly tetrahedral carbon films. The filtered cathodic vacuum arc (FCVA) gives tetrahedral amorphous carbon (ta-C) and the electron cyclotron wave resonance (ECWR) produces the hydrogenated counterpart, ta-C:H. The other method we adopted, a DC sputtering system, is more suitable for the production of sp^2 bonded amorphous carbon. In all cases the samples were deposited at room temperature on high resistive silicon substrates.

2.1. Plasma deposited a-C:N:H

The a-C:N:H films were deposited by decomposition of two different gas mixtures of N_2/C_2H_2 and N_2/CH_4. The films obtained from N_2/C_2H_2 were deposited at ion energy of 80 eV. For the N_2/CH_4 samples the ion energy was decreased to 40 eV to minimize chemical sputtering of the carbon film by the impinging N ions. The pressure prior to deposition was always less than 5×10^{-4} Pa, and during deposition remained below 5×10^{-2} Pa. However, small variations occurred as the nitrogen to hydrocarbon gas ratio was varied from 0 to 7, when using N_2/C_2H_2, and from 0 to 15, when using N_2/CH_4. Methane was used in instead of acetylene to produce a-C:N:H samples with a higher H% [24].

2.2. Dual ion beam a-C:N

Hydrogen free samples were obtained by a dual ion beam approach, where an ECWR source provided a beam of N ions and the carbon ions were produced in a FCVA system. The pressure was maintained below 5×10^{-2} Pa during deposition to maximize the ion current density of both beams. The N ion energy was

between 60 and 100 eV, sufficiently high to allow subplantation but not too high to cause significant chemical sputtering [12,25].

2.3. DC sputtering system

In contrast to the previous deposition methods, the sputtering system operates at relative higher pressures (~4 Pa). The a-C:N films were deposited by sputtering a graphite cathode in argon–nitrogen atmosphere. By setting the percentage of nitrogen gas in the mixture to 0, 25, 50, 75 and 100% the nitrogen content of the films could be changed. The other deposition parameters were kept fixed.

2.4. Characterization

The IR spectra were measured in the 400–4000 cm^{-1} range. An average of 200 scans were taken per sample whilst purging the spectrometer with nitrogen to reduce the signal from water vapor and CO_2. Unpolarized Raman spectra were recorded ex situ at room temperature in backscattering geometry using a variety of Renishaw Raman spectrometers adapted to work with excitation wavelengths varying from 244 to 785 nm. Care was taken to avoid sample damage.

The N/C ratios were obtained by EELS using a Vacuum generator HB501 scanning transmission electron microscope with a dedicated parallel EELS spectrometer. The Samples for EELS were 30–50 nm thick and deposited on silicon substrates. To remove the films from the substrates, the samples were immersed in a solution of $HF:HNO_3:H_2O$ which etches the silicon substrate but does not affect the film. Once the silicon has been etched away, the films floated to the surface and the film was transfer to a 200-mesh microscopy grid. For some of the hydrogenated samples, elastic recoil detection analysis and Rutherford backscattering were used to determine the hydrogen content. These films have been extensively characterized and other relevant results can be found in Refs [12,22–25].

3. IR spectra classification

We propose to classify the IR spectra of CNs, according to four characteristics 'shapes', as shown in Fig. 1. The IR spectra of a-C:N:H samples can be divided into two different groups. The first one, ta-C:N:H, includes all the hydrogenated samples deposited with ion bombardment, i.e. those deposited on the cathode of a PECVD system subject to a substrate bias [26–28], or ta-C:H:N samples deposited with an ECWR from a gas mixture of acetylene and nitrogen [29]. The second group, a-C:N:H, consists of hydrogenated samples with higher H content (>30 at.%), deposited at lower ener-
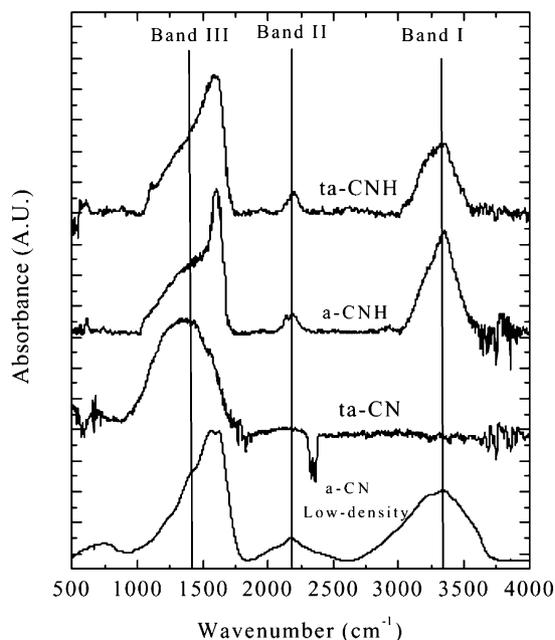
Fig. 1. Four characteristic 'shapes' of the IR absorption of amorphous CN.

gies [30,31] such as those we deposited from a gas mixture of methane and nitrogen. The third type corresponds to CN samples prepared by PVD techniques with ion bombardment, which do not directly introduce H, and therefore produce hydrogen-free CN samples. This group includes all FCVA (t)a-C:N samples; a-C:N deposited using unbalanced magnetron sputtering systems or dual ion beams [32–36], or any other PVD system that promotes ion bombardment. Finally, the fourth type is a peculiar group of CN samples which, independent of the deposition process, have the IR spectra in the 3000–3300 cm^{-1} region dominated by hydrogen related bands, even though H was not necessarily present during the deposition [37–41]. These four types cover all of the different shapes of IR spectra seen in literature, with very few exceptions [42,43]. In these exceptions a strong band at 1100 cm^{-1} is sometimes found and assigned to C–N single bonds. However, this could equally be due to silicon inclusion as shown in Ref. [44].

The fourth type deserves special attention, since it has been shown that, for some CN films, water is easily absorbed from the environment [45]. Water is mainly incorporated through the formation of hydrogen bonds either between H and O (N–H…O) or between H and N (O–H…N) producing a broad IR signal, which can extend from 2000 to 3600 cm^{-1}. Obviously, poor vacuum conditions during deposition can also lead to moisture contamination and then clear NH or OH bonds are formed. The evolution of the IR spectra of the CN samples after exposure to air can be used to differentiate between water absorption [41] and contamination. However, the shape of the OH stretching band (broader and extended to smaller wave numbers) and the density of the films can also help to distinguish between the two phenomena. A low-density is a requisite for the formation of hydrogen bonding, since it is a long directional bond that needs sufficient space to be accommodated [46]. From hereon, this fourth type of samples will be referred as low-density, high-porosity a-C:N. The films are typically soft, easily scratched and present a rough surface characteristic of columnar growth. A relatively high nitrogen content can be achieved in these samples, ∼40 at.% and their Raman spectra are characterized by a high photoluminescence background. Their IR spectra look similar to the ones of hydrogenated CN films, even if H was not directly incorporated.

These four IR shapes and the structural properties given later can be used to characterize and distinguish between different a-C:N and a-C:N:H films.

The IR spectra in Fig. 1 are divided in three different spectral regions I, II and III, broadly corresponding to 2900–3600 cm^{-1}, 2000–2500 cm^{-1} and 1000–2000 cm^{-1}.

Band I arises from NH and/or OH stretching vibrations. Band II is due to C≡N, N≡C and/or –N=C=N– groups. There is no question about these assignments, confirmed also by ^{15}N and D substitutions [19,20,45]. The origin of band III is the subject of this paper.

One approach was to assume that the band III was a convolution of C–N (1100–1300 cm^{-1}) and C=N bonds (1500–1600 cm^{-1}) [47]. Had this been true, it would have greatly facilitated the identification of the predominant bonding in the films [48]. However, if this were the case, isotopic ^{15}N substitution should create a shift in the position of band III. Kaufman et al. [19] showed that there was no shift. Therefore, Band III cannot be directly related to molecular-like CN bonds [19,20,45]. This simple observation invalidates the many claims of deposition of CN films with a high fraction of CN single bonds, based on IR analysis using the assumptions of Friedrich [47], such as in Refs [49,50].

Another common idea is that pure carbon films are transparent at the IR frequencies, showing no absorption bands [19]. Therefore, the appearance of a strong IR absorption in the CN films was thought to be necessarily a consequence of the introduction of nitrogen into the carbon network [19]. Thus, band III should be due to Raman CC vibrations activated in the IR by the N inclusion, since N would break the symmetry of the aromatic rings [19]. These ideas are widely accepted and many explain band III as due to the activation of the D and G Raman modes in the IR.

However, some simple arguments can be put forth to show that this commonly accepted interpretation is incorrect:
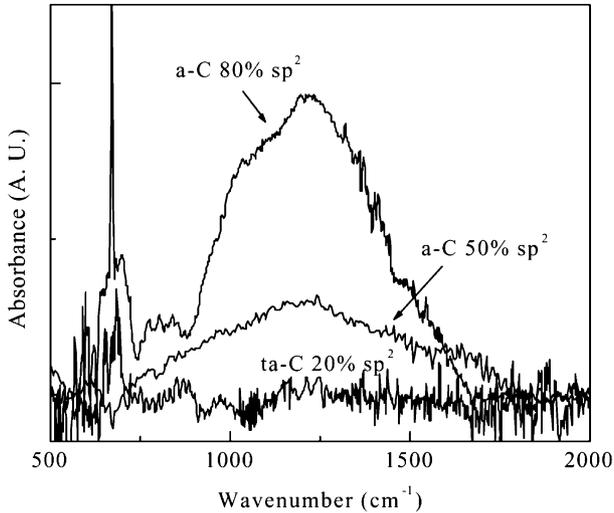
Fig. 2. IR absorption of pure carbon films, no nitrogen added. The intensity has been normalized to take into account the film thickness.

1. Pure carbon films in fact show a non-negligible, and sometimes very intense, IR absorption band in the same region III, Fig. 2. Therefore, there is no requirement for nitrogen to induce the IR activity.
2. Visible Raman and IR spectra of CN films can sometimes be similar in shape only for hydrogenated CN films or for the low-density CN films, but not for ta-C:N or high-density a-C:N films, as clearly shown in Fig. 3 and Ref. [20].
3. Even if sometimes the spectral shapes can look similar, the fitted trends of the G and D peaks in Raman and IR spectra are often different and sometimes even opposite [51].
4. Finally, the strongest argument is that Raman spectra of carbon films are always resonant at any excitation energy [52–54], and their shape change with energy. So any similarity between the Raman spectra at some excitation energy (such as visible Raman) and the IR spectra is a-priori merely a coincidence.

In the following sections we will first analyze the IR spectra of the various N-free amorphous carbons in the sub 2000 cm^{-1} region. Then, we propose a new explanation for the IR activity in this spectral region. Next, we present the dispersion of the Raman features for different CN films. And, finally consider the effect of nitrogen introduction on the IR spectra showing that the same principles used to explain the IR activity in N-free samples can be used to explain the spectra in CN films.

4. IR spectra of nitrogen-free carbon films

Most of the work on carbon films has focused on the heteroatom vibrations in the IR spectra, i.e., the CH vibrations [55,56]. Skeletal CC vibrations are often neglected. However, the IR spectrum of evaporated

(sp^2) a-C was measured by Knoll and Geiger [57], who found peaks at ∼700, 1300 and 1500 cm^{-1}. For diamond-like carbons, Theye et al. [58] investigated in detail the sub 2000 cm^{-1} region for polymeric and diamond-like a-C:H. They studied the effect of deuterium substitution and annealing up to 600 °C. With the deuterium substitution, they observed two broad bands (1350–1400 cm^{-1} and 1550–1580 cm^{-1}) clearly due to skeletal CC vibrations, since all the CH bending modes were shifted away from that region. On the other part, it is well known that annealing a-C:H films above 600 °C removes H, increases the sp^2 fraction and the π delocalization. Theye's work [58] shows that there was also an increase in the IR intensity approximately 1350 cm^{-1}, resulting in a spectrum very similar to the H-free carbon films [57], more recently reported by Bonelli et al. [59] and Rodil et al. [24]. Fig. 2 compares the normalized IR spectra of a ta-C sample (20% sp^2), a ∼50% sp^2 a-C sample and a sputtered a-C sample (80% sp^2). The intensity is in arbitrary units, however the absorption in the low sp^3 films is comparable to that observed in some CN films of similar thickness. It can be seen that only the highest sp^3% ta-C has negligible IR absorption. However, for lower sp^3 contents a clear IR absorption is detected, increasing for decreasing sp^3 fraction. Fig. 2 and Theye's results [58] suggests that the IR absorption in the 1000–2000 cm^{-1} region is only due to the CC sp^2 phase and it is responsible for the variation in the observed spectra. Neglecting the sp^3 phase, the sp^2 phase can be regarded as a mixture of chains and rings of different size, order and relative proportion. We can thus adopt a molecular approach to simply describe the IR activity of the sp^2 phase. The IR intensity of the band corresponding to the normal mode
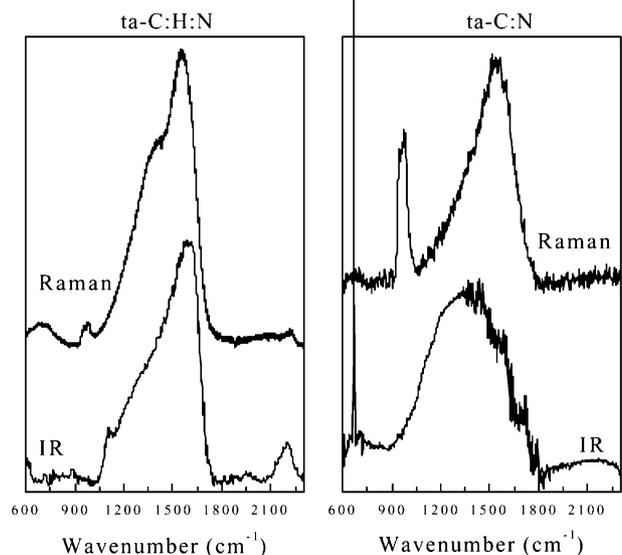

Fig. 3. Comparison between the IR and Raman spectra of hydrogenated and non-hydrogenated CN films.

Q_i is related to the IR effective charge, e^*. e^* is given by change in the dipole-moment μ during the vibration [60–62].

$$I \propto (e^*)^2 = \left| \frac{\partial \mu}{\partial Q_i} \right|^2 \qquad (1)$$

The dipole-moment can be written as:

$$\mu = \sum_\alpha q_\alpha \mathbf{r}_\alpha \qquad (2)$$

where the charge q_α on atom α may change during the vibration. We therefore have:

$$e^* = \frac{\partial \mu}{\partial Q_i} = \sum_\alpha \left(\frac{\partial q_\alpha}{\partial Q_i} \mathbf{r}_\alpha + q_\alpha \frac{\partial \mathbf{r}_\alpha}{\partial Q_i} \right) \qquad (3)$$

For H and N free samples we can assume $q_\alpha = 0$ at the equilibrium position as for any homopolar solid, then the second term in Eq. (3) is 0. However, the first term can be non-zero. It is called the dynamic charge in solid state or the charge flux in the chemical literature [60–62].

$$e^* = \frac{\partial \mu}{\partial Q_i} \approx \sum_\alpha \frac{\partial q_\alpha}{\partial Q_i} \mathbf{r}_\alpha \qquad (4)$$

The main contribution to IR intensity will therefore be the dynamic charge or charge fluxes $\partial q_\alpha / \partial Q_i$. The charge flux accompanying a normal mode Q_i can be expressed as [60–62]:

$$e^* = \sum_e \mu^{ge} \frac{\left\langle e \left| \frac{\partial H}{\partial Q_i} \right| g \right\rangle}{E_e - E_g} \qquad (5)$$

where $\partial H / \partial Q_i$ is the electron phonon coupling term, g is the ground state and e the excited state.

In a crystalline homopolar solid with two or less atoms per unit cell, e^* is 0 by symmetry, because the contribution from each bond about any atom add up to 0. In a homopolar random network, a crystal with three or more atoms per cell, or molecule, e^* can be non-zero. Eq. (5) shows that e^* varies inversely with the average band gap. In highly sp^3 bonded carbon films, the σ bonds have a much wider band gap, so they are less polarisable, and their IR activity is much less. Furthermore, e^* and the IR absorption is much larger in sp^2 a-C than ta-C for two reasons. The π states have a smaller energy gap $E_e - E_g$ than the σ bonds, and secondly the conjugated π bonding of sp^2 sites means that there can be long-range charge flow over a number of bonds, so that e^* increases with delocalization [60–62]. Both these effects give a much larger dynamic charge for π states.

We therefore propose that the main reason for the increase in the IR activity in higher sp^2 samples is the presence of the system of delocalized π bonds with increasing conjugation. Indeed, in ta-C the residual sp^2 phase has very localized π bonds [63], thus the IR activity is negligible, as seen in Fig. 2. Indeed, the main effect is passing from a localized π-system to a longer, delocalized one. The higher fraction of the sp^2 phase with higher electron delocalization allows higher charge fluxes and thus higher IR activity.

5. Resonant Raman spectra of amorphous CNs

In this section we will present the resonant Raman scattering from our CN films. It will be clear how peak positions and intensities change with excitation energy. This only is sufficient to indicate that the apparent similarity between a Raman spectrum taken at some excitation energy and an IR spectrum, in particular the presence of two main peaks, is a priori purely accidental.

Raman scattering from carbon is always a resonant process. The configurations that are preferentially excited are those whose band gap matches the excitation energy used. Any mixture of sp^3, sp^2 and sp^1 carbon atoms always has a gap between 0 and 5.5 eV, and this energy range matches that of IR–vis–UV Raman systems [54]. The Raman spectra of all carbon films show several common features: the so-called G and D peaks, which lie at approximately 1560 and 1360 cm^{-1} for visible excitation, and the T peak, seen for UV excitation, at approximately 1060 cm^{-1}. The G and D peaks are due to sp^2 sites only. The G peak is due to the bond stretching of all pairs of sp^2 atoms in both rings and chains [64]. The D peak is due to the breathing modes of sp^2 atoms in rings. The T peak is due to the C–C sp^3 vibrations but is only seen using UV excitation.

Most of the previous literature, in the quest for C_3N_4, was pressed by the need of finding identifiable signatures for C–N bonds [65] or N=N bonds [66] in the Raman and FTIR spectra. This biased approach was the main cause for errors and unsound conclusions. Indeed, the Raman spectra of CN films resembles that of pure carbon films and ^{15}N substitution suggests no direct detectable contributions from CN nor NN bonds in the 1000–2000 cm^{-1} spectral region [23]. To interpret the resonant Raman spectra of CN films we thus adopt the same approach used for single wavelength excitation [22], i.e. analyzing the trends in the G and D positions in the same way as for N-free samples [22].

The Raman spectra and their dispersion are characteristic of each type of carbon, while their single wavelength Raman spectrum may be indistinguishable [54,64]. The G (or D) dispersion, i.e. the slope of the wavelength dependence of the peak frequency [54], is a good indicator of the degree of disorder.

Figs. 4 and 5 show the multi-wavelength (MW) Raman spectra of an a-C:N sample and a ta-C:N:H sample, respectively. The spectra change with the incident laser wavelength. To obtain the positions and
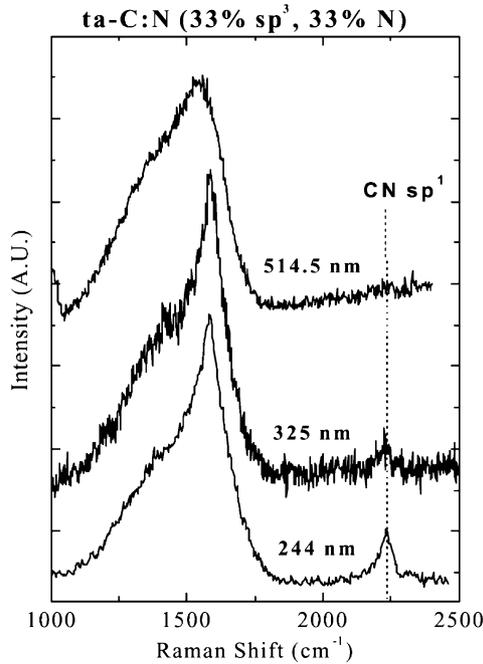
Fig. 4. Raman spectra of a ta-C:N sample measured at different excitation wavelengths. Notice how the 'shape' of the spectra changes with the laser wavelength. CN–sp[1] bonds are remarkably enhanced for UV–Raman.

intensities of the G and D peaks, we fitted the spectra using a combination of a Breit–Wigner–Fano and a Lorentzian for the G and D peaks. Fig. 6 shows the variation of the G peak position as a function of the excitation wavelength. The G band downshifts with decreasing exciting wavelength. The slope of the linearly fit of Fig. 6 gives the G dispersion (cm^{-1}/nm) and is proportional to the degree of disorder [54]. A complete analysis of the MW Raman data is reported elsewhere [23]. In this paper we mainly wish to show that Raman scattering in CN films is a resonant phenomenon and therefore the shape of the spectra depends on the exciting energy. Thus the similarity between IR and visible Raman spectra of CNs is not enough argument to prove that the vibrations observed in the IR spectra have the same origin than the D and G Raman bands of amorphous carbon films.

6. Effect of nitrogen inclusion into carbon films

In this section a review of the experimental results on the effects of nitrogen inclusion into the different carbon networks is presented. The starting N-free film can be anywhere in the ternary phase diagram for carbon films, Fig. 1 on Ref. [67]. In general, in high sp^3 carbon films, the effect of N is to reduce the number of carbon atoms with tetrahedral bonding. This result is general and applies to hydrogenated and non-hydrogenated films, as seen in Fig. 7. This trend is different for
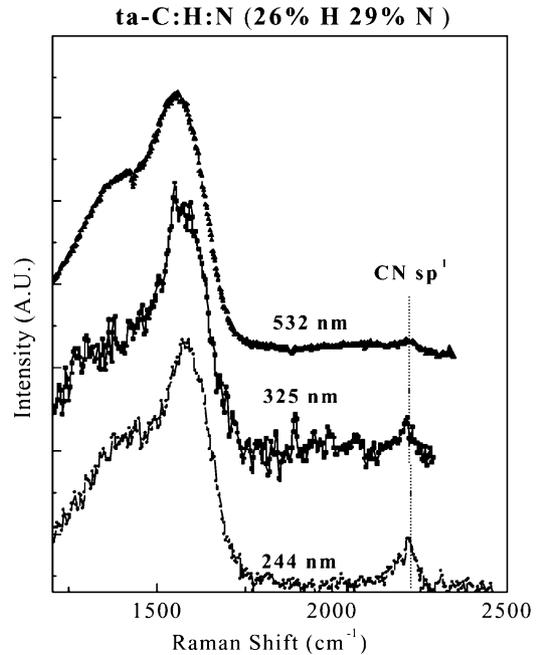

Fig. 5. MW Raman spectra for hydrogenated CN films. Note that again CN–sp[1] bonds are clearly detected at UV–excitation.

sputtered samples deposited at substrate temperatures above 200 °C [34]. Unfortunately, there is no information on the sp^3 content of this kind of samples, but the apparent increase of hardness and other mechanical properties with nitrogen addition suggests a small increase in the sp^3 content [68]. We will not further discuss this type of films since here we concentrate on room temperature prepared CN films.

The effect of the nitrogen content on the IR spectra and the optical gap can be seen in Figs. 8 and 9. These figures show the integrated IR activity in the 1000–1800 cm^{-1} region as a function of N and sp^2 content.
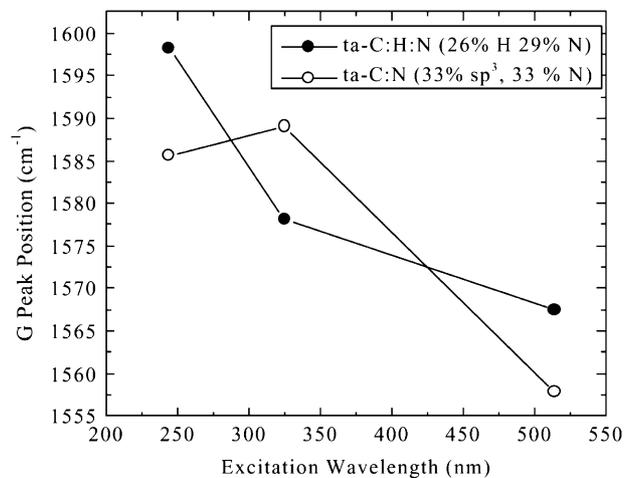

Fig. 6. Dispersion of G peak vs excitation wavelength for a representative sample of ta-C:N and ta-C:H:N.
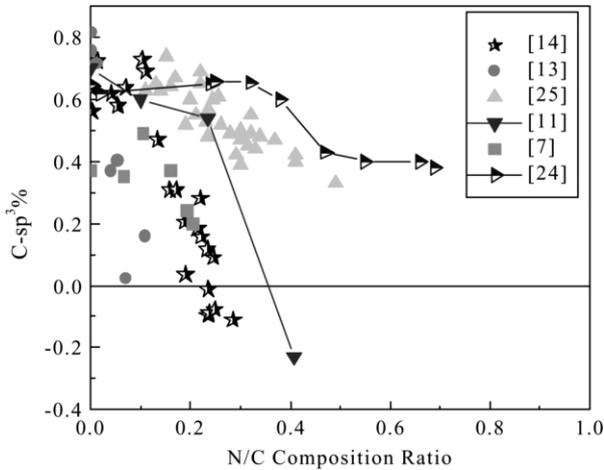
Fig. 7. Variation of the C–C sp^3 fraction as measured by EELS. Negative values in the sp^3 fraction are indicative of a significant fraction of sp^1 bonds. These are usually neglected in the standard C–sp^3 calculations because carbon films hardly content any CC–sp^1 bonds. However, IR and Raman spectra of CN films clearly show the presence of CN–sp^1 bonds.

Previous to the integration the IR spectra were normalized to the thickness of each sample, so that the integrated area is a true estimation of the IR absorption. In general, there is an increment in the integrated area of band III as both nitrogen content and sp^2 fraction increase, whilst the optical gap decreases.

Figs. 8 and 9 also show that the integrated IR intensity is a very useful parameter to characterize CN samples, even though it is rarely considered in the literature. The precise trends may vary for specific samples or deposition systems [69], but here we just want to show the main parameters controlling (sp^2% and average band-
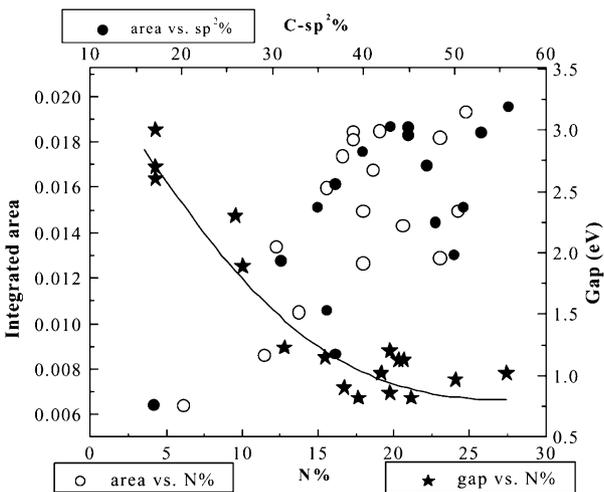

Fig. 9. Tauc optical gaps (right: *y*-axis) and IR integrated area from 900 to 1800 cm^{-1} vs. nitrogen content (bottom: *x*-axis) and vs. CC-sp^2% (top: *x*-axis). Corresponding to the series of hydrogenated samples deposited by a mixture of C_2H_2/N_2. The line is only a guide for the eyes.

gap) the IR spectra in the general classes of amorphous CNs and Figs. 8 and 9 are sufficient to support our views.

Fig. 8. Tauc optical gaps (right: *y*-axis) and IR integrated area from 900 to 1800 cm^{-1} vs. nitrogen content (bottom: *x*-axis) and vs. CC-sp^2% (top: *x*-axis). Corresponding to a series of ta-C:N samples. The line is only a guide for the eyes.
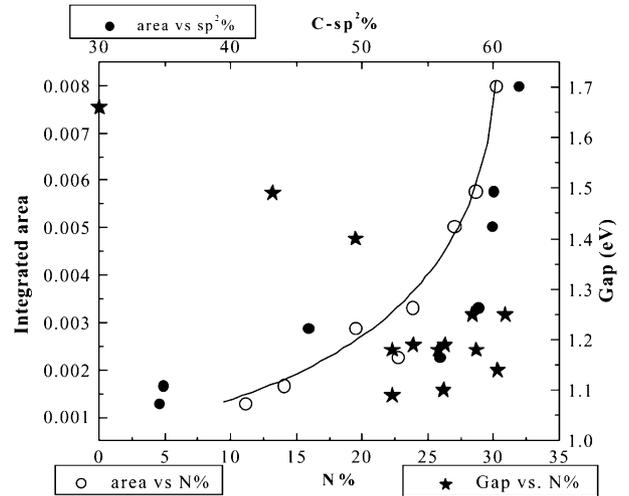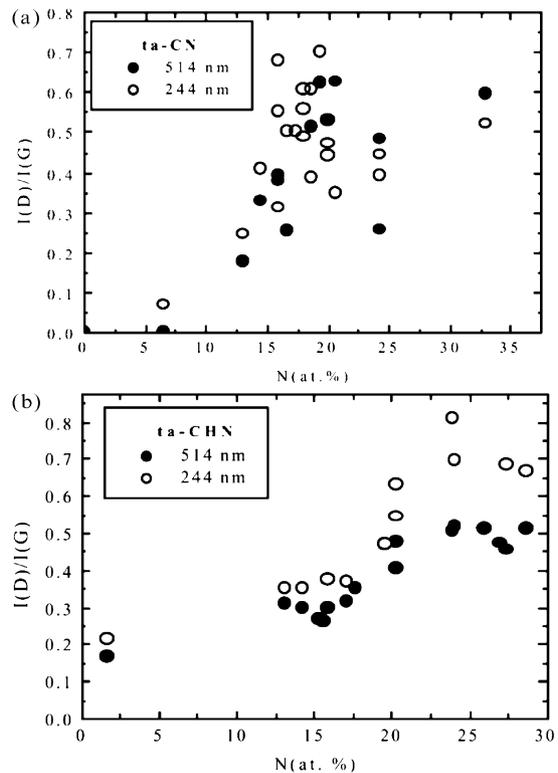

Fig. 10. $I(D)/I(G)$ intensity ratios vs. Nitrogen content for two different excitation wavelengths. (a) ta-C:N samples and (b) ta-C:H:N samples.
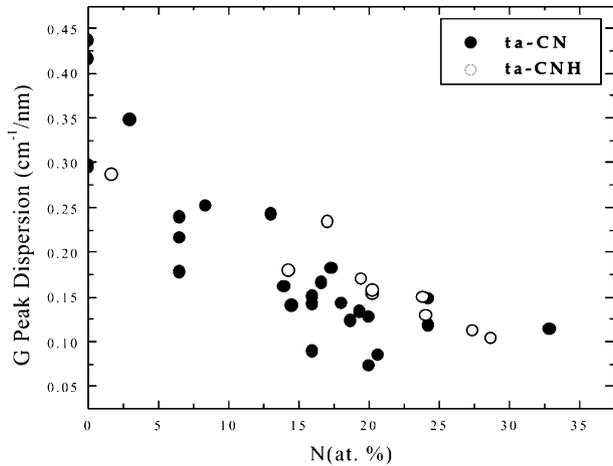
Fig. 11. G peak dispersion for both ta-C:N and ta-C:H:N samples at increasing nitrogen content. The y-axis is the slope (in cm^{-1}/nm) of the linear fit to the G position vs. the three excitation wavelengths for the samples shown in Fig. 6. Similarly, the G dispersion was calculated for the remaining nitrogen content films, not shown in Fig. 6.

Generally, the introduction of nitrogen directly induces an increase and clustering of the sp^2 phase and only indirectly modifies the Raman spectra. This is clearly seen in Figs. 10 and 11. Fig. 10 shows that the I(D)/I(G) ratio increases as a function of N content for both 514.5 and 244 nm excitation wavelengths [23], indicating clustering of the sp^2 phase [64]. Fig. 11 shows the G peak dispersion as a function of N content for (t)a-C:N and (t)a-C:N:H samples. For any film, the G peak dispersion decreases with nitrogen content, suggesting again ordering of the sp^2 phase, in agreement with the sp^2 clustering evidenced in Fig. 10. Spectra from the sputtered samples are more difficult to analyze due to the strong photoluminescence signal.

7. Conclusions

The results of Sections 4–6 allow us to propose a new mechanism to explain the origin of the bands in the IR spectra in amorphous carbon and amorphous CN. It is clear that it is only the sp^2 phase that is responsible for the observed spectra. The higher the fraction of the sp^2 phase having greater electron delocalization promotes charge fluxes within the molecule and thus higher IR absorption.

As mentioned in Section 6, N introduction increases the C-sp^2 fraction (either by forming C=N or inducing C=C bond formation) and the clustering of the sp^2 phase and this alone, as explained in Section 4, increases the IR absorption. Furthermore, nitrogen increases the static charge on the carbon atoms to which N is bonded and, due to the presence of the π-system, the polarization of the sp^2 skeleton, thus resulting in an additional increase in the charge fluxes. This can be understood if one considers that N, even if not directly contributing

an extra electron to the π-system, polarizes all the sp^2 bonds of the conjugated system to which this is a terminal atom. Thus N increases the bond dipole moment of each CC bond resulting in an effect that is greater the longer the conjugated chain.

We believe that the effect of N introduction in amorphous carbons parallels the effects of doping in polyconjugated materials, such as polyenes and polyaromatic polyconjugated polymers [60,70–72]. For these conjugated systems a noticeable facet of the IR spectra is that some bands in the fingerprint region (1700–900 cm^{-1}) have IR peaks one or two orders of magnitude higher than the corresponding bands of the neutral species. These strong IR intensities in general cannot be explained only in terms of the static polarization of the relevant bonds, and hence some intimate interplay between the vibrational and electronic processes is necessary for the generation of such strong IR intensities [73]. The mechanism that gives rise to the strong IR intensities can be easily explained for charged linear polyenes [74,75]. A simple model includes two valence-bond resonance structures in which an electric charge resides on either end of the conjugated chain. The location of the electronic charge and the bond alternation pattern in one of the resonance structures is opposite from those in the other. As a consequence, adjacent CC bonds stretch and contract alternately and the electric charge moves from one end to the other upon the transition between the two resonance states. In other words, the electric charge moves through the conjugated chain by the vibration along the bond alternation coordinate. However, for molecules with an intricate network of chemical bonds, such as polycyclic aromatic hydrocarbons, a more general theoretical formulation is needed to explain the IR activity, since the vibrational patterns cannot be anticipated from the molecular structures alone [76,77]. Two facts have been determined, one that CC bond stretching is mainly responsible for the IR activity and, secondly, that the vibrational motions are closely related to the electronic structure. The enhancement of the strong IR bands is believed to occur through a mechanism of charge fluxes, both long-range (between rings), as well as, that of short-range (intra-ring). Both mechanisms are related to electron–vibration interactions that involve only π electrons.

A similar interpretation of the IR spectra of CN films has been recently given by Franchini et al. [21,78]. They proposed that the dipolar field generated by CN sp^1 groups polarizes the π-electrons of the sp^2 clusters to which they are bonded, so that IR active C=C stretching modes appear in the clusters. This implicitly means that N is necessary to induce the IR activity in the 1000–1800 cm^{-1} region. In contrast, we proposed that it is the charge flux in the complex conjugated system formed by alternation of C=C and C=N (both in rings and chains) that is responsible for the strong IR

activity in carbon and CN films.

References

[1] A.Y. Liu, M.L. Cohen, Science 245 (1989) 841.
[2] S. Matsumoto, E.Q. Xie, F. Izumi, Diamond Relat. Mater. 8 (1999) 1175.
[3] S. Muhl, J.M. Méndez, Diamond Relat. Mater. 8 (1999) 1809.
[4] T. Malkow, Mater. Sci. Eng., A 292 (2000) 112.
[5] L.M. Zambov, C. Popov, N. Abedinov, M.F. Plass, W. Kulish, T. Gotszalk, P. Grabiec, I.W. Rangelow, R. Kassing, Adv. Mater. 12 (2000) 656.
[6] T.A. Yeh, C.L. Lin, J.M. Sivertsen, J.H. Judy, IEEE Trans. Magn. 27 (1991) 5163.
[7] S.R.P. Silva, J. Robertson, G.A.J. Amaratunga, B. Rafferty, L.M. Brown, J. Schwan, D.F. Franceschini, G. Mariotto, J. Appl. Phys. 81 (1997) 2626.
[8] C. Ronning, H. Feldermann, R. Merk, H. Hofsass, P. Reinke, J.U. Thiele, Phys. Rev. B 58 (1998) 2207.
[9] J.M. Ripalda, E. Román, I. Montero, G. Comelli, A. Baraldi, S. Lizziti, A. Goldoni, G. Paolucci, Phys. Rev. B 60 (1999) 3705.
[10] W.T. Zheng, K.Z. Xing, N. Hellgren, M. Logdlund, A. Johansson, U. Geliivs, W.R. Salaneck, J.E. Sundgren, J. Electr. Spectr. Relat. Phenomena 87 (1997) 45.
[11] S. Bhattacharyya, M. Hietschold, F. Richter, Diamond Relat. Mater. 9 (2000) 544.
[12] S.E. Rodil, W.I. Milne, J. Robertson, L.M. Brown, Diamond Relat. Mater. 10 (2001) 1125.
[13] C.A. Davis, D.R. Mackenzie, Y. Yin, E. Kravtchinskaia, G.A.J. Amaratunga, V.S. Veerasamy, Phil. Mag. B 69 (1994) 1133.
[14] J. Hu, P. Yang, C.M. Lieber, Phys. Rev. B 57 (1998) 3185.
[15] I. Jímenez, R. Gago, J.M. Abella, L.J. Terminello, Diamond Relat. Mater. 10 (2001) 1170.
[16] N. Hellgren, J. Guo, C. Sathe, A. Agui, J. Nordgren, Y. Luo, H. Agren, J.E. Sundgren, Appl. Phys. Lett. 79 (2001) 4348.
[17] W.T. Zheng, J.H. Guo, Y. Sakamoto, M. Takaya, X.T. Li, P.J. Chao, Z.S. Jin, K.Z. Xing, J.-E. Sundgren, Diamond Relat. Mater. 10 (2001) 1897.
[18] I. Shimoyama, G. Wu, T. Sekiguchi, Y. Baba, Phys. Rev. B 62 (2000) R6053.
[19] J.H. Kaufman, S. Metin, D.D. Saperstein, Phys. Rev. B 39 (1989) 13053.
[20] N.M. Victoria, P. Hammer, M.C. Dos Santos, F. Alvarez, Phys. Rev. B 61 (2000) 1083.
[21] G. Franchini, A. Tagliaferro, G. Messina, S. Santangelo, A. Paoletti, A. Tucciarone, J. Appl. Phys. 91 (2002) 1155.
[22] S.E. Rodil, A.C. Ferrari, J. Robertson, W.I. Milne, J. Appl. Phys. 89 (2001) 5425.
[23] A.C. Ferrari, S.E. Rodil, J. Robertson, Phys. Rev. B, submitted for publication.
[24] (a) S.E. Rodil, N.A. Morrison, J. Robertson, W.I. Milne, Phys. Status Solidi. A 174 (1999) 25(b) S.E. Rodil, Ph.D. Thesis, University of Cambridge, 2000.
[25] S.E. Rodil, W.I. Milne, J. Robertson, L.M. Brown, Appl. Phys. Lett. 77 (2000) 1458.
[26] K.J. Clay, S.P. Speakman, G.A.J. Amaratunga, S.R.P. Silva, J. Appl. Phys. 79 (1996) 7227.
[27] J. Schwan, V. Batori, S. Ulrich, H. Ehrhardt, S.R.P. Silva, J. Appl. Phys. 84 (1998) 2071.
[28] P. Hammer, N.M. Victoria, F. Alvarez, J. Vac. Sci. Technol. A 16 (1998) 2941.
[29] S. Rodil, N.A. Morrison, W.I. Milne, J. Robertson, V. Stolojan, D.N. Jayawardane, Diamond Relat. Mater. 9 (2000) 524.
[30] N. Mutsukura, K. Akita, Thin solid Films 349 (1999) 115.
[31] M. Zhang, Y. Nakayama, T. Miyazaki, M. Kume, J. Appl. Phys. 85 (1999) 2904.
[32] V. Hajek, K. Rusnak, J. Vleck, L. Martinu, S.C. Gujhrati, J. Vac. Sci. Technol. A 17 (1999) 899.
[33] R. Kaltofen, T. Sebald, G. Weise, Thin Solid Films 290 (1996) 112.
[34] N. Hellgren, K. Macak, E. Broitman, M.P. Johansson, L. Hultman, J.-E. Sundgren, J. Appl. Phys. 88 (2000) 103.
[35] S. Kumar, T.L. Tansley, J. Appl. Phys. 76 (1994) 4390.
[36] C. Quirós, P. Prieto, A. Fernández, E. Elizalde, C. Morant, R. Schlögl, O. Spillecke, J.M. Sanz, J. Vac. Sci. Technol. A 18 (2000) 515.
[37] Y. Li, S. Xu, H. Li, W. Lu, J. Mater. Sci. Lett. 17 (1998) 31.
[38] Y. Kusano, J.E. Evetts, R.E. Somekh, I.M. Hutching, Thin Solid Films 332 (1998) 56.
[39] Y.M. Ng, C.W. Ong, X.-A. Zhao, C.L. Choy, J. Vac. Sci. Technol. A 17 (1999) 584.
[40] J.J. Cuomo, D.L. Pappas, R. Lossy, J.P. Doyle, J. Bruley, G.W. Di Bello, W.J. Krakow, J. Vac. Sci. Technol. A 10 (1992) 3414.
[41] L. Maya, J. Poly. Sci. 31 (1993) 2595.
[42] J. Wei, J. Appl. Phys. 89 (2001) 4099.
[43] S. Veprek, J. Weidmann, F. Glatz, J. Vac. Sci. Technol. A 3 (1995) 214.
[44] G. Lehmann, P. Hess, J.J. Wu, C.T. Wu, T.S. Wong, K.H. Chen, L.C. Chen, H.Y. Lee, M. Amkreutz, Th. Frauenheim, Phys. Rev. B 64 (2001) 165305.
[45] F. Alvarez, N.M. Victoria, P. Hammer, F.J. Freire, M.C. dos Santos, Appl. Phys. Lett. 73 (1998) 1065.
[46] N.B. Colthup, L.H. Daly, S.E. Weberley, Introduction to IR and Raman Spectroscopy, third ed., Academic Press, NY, 1990.
[47] M. Friedrich, Th. Welzel, R. Rochotxki, H. Kupfer, D.R.T. Zahn, Diamond Relat. Mater. 6 (1997) 33.
[48] D. Lin-Bien, N.B. Colthup, W.G. Fateley, J.G. Grasselli, The Handbook of Infrared and Raman Frequencies of Organic Molecules, Academic press, NY, 1991.
[49] Y.K. Yap, S. Kida, T. Aoyama, Y. Mori, T. Sasaki, Diamond Relat. Mater. 8 (1999) 614.
[50] A. Laskarakis, S. Logothetidis, M. Gioti, Phys. Rev. B 64 (2001) 125419.
[51] J.M. Méndez, A. Gaona-Cuoto, S. Muhl, S. Jiménez-Sandoval, J. Phys.: Condens. Matter 11 (1999) 5225.
[52] M.A. Tamor, J.A. Haire, C.H. Wu, K.C. Hass, Appl. Phys. Lett. 54 (1989) 123.
[53] I. Pocsik, M. Koos, M. Hundhausen, L. Ley, in: S.R.P. Silva, et al. (Eds.), Amorphous Carbon: State of the Art, Word Scientific, Singapore, 1998, p. 224.
[54] A.C. Ferrari, J. Robertson, Phys. Rev. B 64 (2001) 075414.
[55] B. Dishler, Europ. Mater. Res. Soc. Symp. Proc. 17 (1987) 189.
[56] J. Ristein, R.T. Stief, L. Ley, W. Beyer, J. Appl. Phys. 84 (1998) 3836.
[57] J. Knoll, J. Geiger, Phys. Rev. B 29 (1984) 5651.
[58] (a) M.L. Theye, V. Paret, A. Sadki, Diamond Relat. Mater. 10 (2001) 182.
(b) Y. Bounouh, M.L. Theye, A. Dehbi-Alaoui, A. Matthewa, J.P. Stoquert, Phys. Rev. B 51 (1995) 9597.
(c) V. Paret, These de Doctorat, Université Pierre et Marie Curie, 1999.
[59] M. Bonelli, A.C. Ferrari, A.P. Fioravanti, A. Miotello, P.M. Ossi, Mat. Res. Soc. Symp. Proc. 593 (1999) 359.
[60] M. Gussoni, C. Castiglioni, G. Zerbi, in: R.J. Clark, R.E. Hester (Eds.), Spectroscopy of Advanced Materials, Wiley, 1991, p. 251.
[61] J.C. Decius, J. Mol. Spectr. 57 (1975) 348.
[62] U. Dinur, Chem. Phys. Lett. 93 (1982) 253.

[63] C.W. Chen, J. Robertson, J. Non-Cryst. Sol. 227–230 (1998) 602.

[64] A.C. Ferrari, J. Robertson, Phys. Rev. B 61 (2000) 14095.

[65] M.R. Wixom, J. Am. Ceram. Soc. 73 (1990) 1973.

[66] A.K.M.S. Chowdhury, D.C. Cameron, M.S.J. Hashimi, Thin Solid Films 332 (1998) 62.

[67] J. Robertson, Phil. Mag. B 76 (1997) 335.

[68] H. Sjostrom, S. Stafstrom, M. Boman, J.E. Sundgren, Phys. Rev. Lett. 75 (1995) 1336.

[69] S.E. Rodil, S. Muhl, in: S.R.P. Silva (ed.) Properties and Growth of Amorphous Carbon, EMIS DataReviews (INSPEC 2002), in press.

[70] G. Zerbi, M. Gussoni, C. Castiglioni, in: J.L. Bredas, R. Silbey (Eds.), Conjugated Polymers, Kluwer Academic Publisher, 1991, p. 435.

[71] M. Del Zoppo, M. Tommasini, C. Castiglioni, G. Zerbi, Chem. Phys. Lett. 287 (1998) 100.

[72] C. Castiglioni, M. Tommasini, M. Del Zoppo, J. Mol. Struct. 521 (2000) 137.

[73] G. Zerbi, C. Castiglioni, S. Sala, M. Gussoni, Synth. Met. 17 (1987) 293.

[74] H. Torii, M. Tasumi, J. Phys. Chem. B 101 (1997) 466.

[75] H. Torii, K. Furuya, M. Tasumi, J. Phys. Chem. A 102 (1998) 8422.

[76] H. Torii, Y. Ueno, A. Sakamoto, M. Tasumi, J. Phys. Chem. A 103 (1999) 5557.

[77] H. Torii, J. Phys. Chem. A 104 (2000) 413.

[78] G. Fanchini, G. Messina, A. Paoletti, S.C. Ray, S. Santangelo, A. Tagliaferro, A. Tucciarone, Surf. Coat. Technol. 151–152 (2002) 1143.